The Development of Typhoon Image Database with Content-Based Search

Asanobu KITAMOTO
Research and Development Department
National Center for Science Information Systems
2-1-2, Hitotsubashi, Chiyoda-ku, Tokyo 101-8430, Japan
kitamoto@rd.nacsis.ac.jp

Abstract

The purpose of the paper is to develop typhoon image database system that provides content-based search on both text-based and image-based information. In particular the author focuses on the shape and motion information that can be derived from satellite images, which is a challenging subject of research for complex shape and non-rigid motion analysis. Many kinds of algorithms are developed for this purpose, and the author shows the result of similarity-based retrieval of typhoon images.

1 Introduction

For those who are familiar with satellite images, the ”typhoon” is one of the most ”eye-catching” objects in those images. Throughout its life cycle, it evolves from a small cloud cluster to a striking vortex shape. After reaching magnificent big vortex with the crisply rounded eye in the center, it suddenly collapses to a irregular shape (shear pattern) and then die. This change of cloud patterns is an interesting subject of research because of the following reasons.

In the first place, it is practically important, since the intensity or scale of a typhoon is estimated based on its cloud patterns and its past changes. Moreover, the analysis of a typhoon must be quickly completed for weather forecast to prevent disaster caused by untimely warning on severe rain and wind. Hence the automatic analysis of typhoon cloud patterns is practically important for weather forecasters to make prompt decisions based on the result of objective analysis. In the second place, the shape analysis of natural and complex shape such as typhoon cloud patterns is a challenging subject of research. Moreover, the change of cloud shape on the sequence of satellite images taken every one hour is a typical problem of non-rigid motion analysis and tracking. Therefore, the typhoon, as a subject of research, contains many attractive research themes worth challenging.

In particular, this paper focuses on the image database of typhoons, and construct the prototype image database by means of the framework called the hierarchical model of image content elements proposed by the author [9, 7]. In this paper, several algorithms will be explained and they have their own counterparts in some layer in the hierarchical model. Section 2 describes typhoon tracking and cropping (Observation Layer), and next Section 3 shows a modified algorithm for cloud classification (Pixel Layer). In Section 4, we extract shape information of cloud clusters from typhoon imagery using shape decomposition with deformable ellipses (Region Layer). Extracted information is further integrated into graph structure, namely attributed relational graphs, for representing the relationship between cloud clusters (Relation Layer). Finally, the functionality of content-based retrieval system for typhoons is briefly described, from the viewpoint of text-based and image-based retrieval (Semantic Layer). Because this database have many features which this paper is too small to contain, this paper is centered on the overview of the features, and we omit the detail of the algorithm to be described.

2 Datasets

Satellite imagery Satellite imagery used in this paper is taken by Geostationally Meteorological Satellite (GMS) 5, also known as “Himawari.” The position of the satellite is about 36,000km above the equator at 140N. It is equipped with a sensor called VISSR (Visible and Infrared Spin Scan Radiometer) with four bands as shown in Table 1. Usually it operates one observation in one hour, and one observation takes about 25 minutes to have a full picture of the earth.

Table 1: Major Characteristics of VISSR.

Band	Wavelength	Resolution
Visible	$0.55 \sim 0.90\mu m$	1.25km
IR1	$10.5 \sim 11.5\mu m$	5.0km
IR2	$11.5 \sim 12.5\mu m$	5.0km
IR3 (Water Vapor)	$6.5 \sim 7.0\mu m$	5.0km

Best Track Typhoon is a regional term given to those mature tropical cyclones that originate in the western north pacific ocean [11]. For all the typhoons after 1951, the official record of typhoons are compiled by the Japan Meteorological Agency (JMA) as "Best Track" dataset, and can be purchased from the Japan Meteorological Business Support Center (JMBSC) with minimum cost. It contains records such as center location, central pressure, and maximum wind in every one to six hours. This dataset especially plays an important role in this paper, because the tracking of typhoon is not an easy task, as it might seem to be, even for well-trained professionals.

Meteorological Surface Observations JMA operates mesoscale observation network called the AMeDAS (Automated Meteorological Data Acquisition System). This system consists of over 1300 observing stations with the mean spatial intervals of 17 km. All stations monitor hourly precipitation, and more than 800 stations monitor air temperature, wind direction/speed, and sunshine duration. Integrating surface observations with satellite observations makes the system even more powerful, since the former provides important information that cannot be obtained from the latter. For example, it is possible to relate the amount of rainfall with satellite cloud patterns.

3 Tracking and Cropping

3.1 Typhoon Tracking

The tracking of a typhoon, namely the center of a typhoon, is generally not an easy task even for well-trained professionals. The eye serves as a landmark for the center in some cases, but in other cases it does not appear on satellite images. Moreover, promptitude is of importance in weather forecast; to finish the analysis in time is important, even if available information is insufficient for the accurate determination of center location. If it is a difficult problem even for well-trained professionals, it is for computer programs also.

Now best track dataset solves this problem, because the records in the dataset are determined after deliberate investigation in the life cycle of a typhoon, hence keep accuracy enough for official use. However, the frequency of best track record is every three to six hours which is not enough to cover the frequency of every one hour satellite observations. We then estimate the position of the typhoon by interpolation; various interpolation methods could be employed for this purpose. To name a few, 1) linear interpolation, 2) spline interpolation, 3) cycloid interpolation, where the last method was used for approximating the eye movement of a typhoon [15]. Considering the purpose of this paper, we decide to use cubic spline interpolation because of its smoothness, although our observations are that linear interpolation does not differ significantly from cubic spline interpolation in most cases.

3.2 Typhoon Cropping

From the original satellite imagery, we then crop typhoon imagery so that the center of the image coincides with the interpolated location of the typhoon. To decide the size of the image, we should remember the fact that supertyphoons have widths of between 600km to 1000km. To include the surrounding regions of the typhoon, we suppose that about the double size of the above figure is the appropriate size for cropped image.

Another design consideration is on geometric correction [6]. In terms of map coordinate system, we select cylindrical equidistant projection, whose advantage is that latitude and longitude of a pixel can be easily calculated from the image coordinate. In addition, nearest neighbor interpolation is used for mapping.

As a result, we decide that the width and height of the image is 512×512 pixels, and the VISSR frame coordinate is mapped onto this image frame so that the width and height corresponds to 25 degrees in longitude and latitude. These figures are determined so that resolution shown in Table 1 matches well to this setting, Figure 1 shows one example and it seems the choice of size is good.

4 Cloud Classification

4.1 Operational Algorithm

The classification here can be crisp or fuzzy, but in any case we should assign some categorical information to each pixel. Our algorithm is based on the operational algorithm used at JMA to make "Satellite Nephanalysis Information Chart (SNIC)" [2]. It takes advantage of multispectral radiometers of VISSR of GMS-5 consisting of Water Vapor (WV) absorption and Split-Window (SP) channels. The clouds are automatically classified into seven classes, namely, cumulonimbus (Cb), cumulus (Cu), cumulus congestus (Cg), cirrus (Ci), stratus / fog (St / Fog), middle layer cloud (Cm), dense cloud (Dense). Because cirrus is usually thin, we also consider mixel-type classes, namely cirrus + middle layer cloud (Ci+Cm), cirrus + cumulus (Ci+Cu).

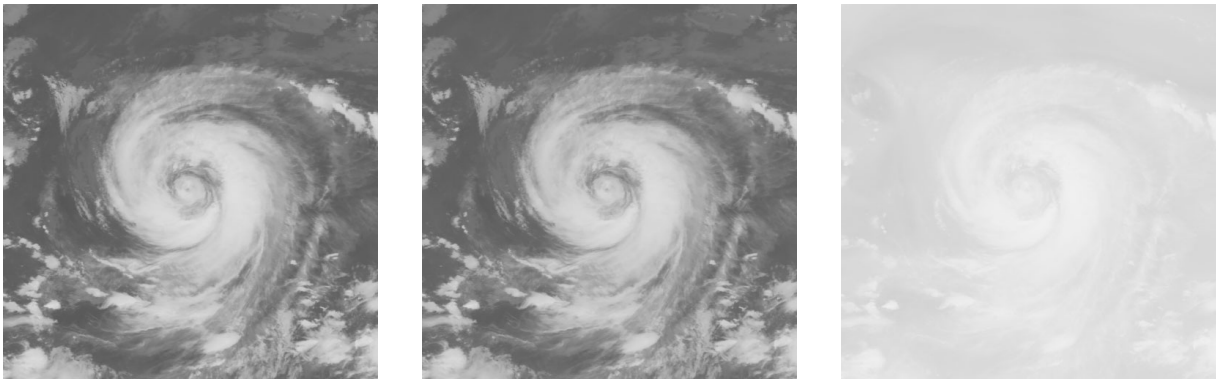

(a) IR1 (b) IR2 (c) IR3 (WV)

Figure 1: Infrared images of Typhoon 9713. These images are taken on UTC 10, August 16, 1997 by GMS 5.

The classifier used at JMA [2] is actually too complex to describe in the limited space. However, the basic principle of the algorithm is to categorize pixels into four layers based on the estimated height. Then each pixel is further classified using another classifier designed for each layer such as "high cloud mode." This method indicates that the estimate of the cloud top height is very important in cloud classification.

However, the operational algorithm cannot be directly used in our system, because several datasets are not available to us. For example, temperature profile, which can be derived as the result of numerical prediction in the form of grid point value (GPV), are not available. Therefore we should develop a new algorithm that can do without those datasets.

4.2 Proposed Algorithm

4.2.1 Surface Temperature

As stated earlier, the most important value to be estimated is cloud top height. However, before estimating this value, we need to know surface temperature and temperature profile in the atmosphere. Temperature profile can be approximated by the U.S. standard atmosphere model, in which temperature decreases with the rate of 6.5K/km as the height increases.

Next we move to the problem of estimating surface temperature from satellite imagery. Now by reminding the fact that a typhoon spends most of its life over the sea, we realize that usually sea surface temperature (SST) should be estimated. One way of estimating SST is to have a database of seasonal and regional average of SST. However, instead of having such a large database, we develop a simple algorithm for estimating latitudinal sea surface temperature.

Firstly, for each horizontal line (same latitude), the temperature of pixels are sorted in descending order and top L percent of pixels are selected for calculating the average of each line. In this paper, $L = 5$. Then the second-order polynomial function is fitted to data points using chi-square fitting [13]. Second-order is chosen because first-order (linear) is too simple, but more than third-order is prone to error. Then cloud top height can be estimated using temperature difference between pixel value and surface temperature under it.

For land surface temperature, we might be able to utilize observed surface temperature from AMeDAS dataset for the land of Japan, however this is left for future work. For other parts of the earth, estimation of land surface temperature is a difficult task, since it shows too much variation in terms of region and time of day compared to sea surface temperature.

4.2.2 Channels Used for Classification

After obtaining the rough estimate of surface temperature and cloud top height, we can classify cloud pixels into 4 layers, namely very high cloud (above 9km), high cloud (5 ~ 9km), middle cloud (1.5 ~ 5km), and low cloud (under 1.5km), and assign the same kind of cloud types used in the operational algorithm according to cloud top height. The definition of cloud types is somewhat arbitrary; however, the most important point in classification is not to mix up cumulus-type, cirrus-type, and other-type clouds, so we try to be precise in terms of this distinction.

The structure of the classifier is a little different from that used in the operational algorithm, since our algorithm does not explicitly separate classifier tree according to the layer of the pixel. Basically we use three (combinations of) channels, namely TBB(IR1), TBB(IR1) - TBB(IR2), TBB(IR1) - TBB(IR3), where TBB means black-body temperature calculated from the digital number of the pixel.

TBB(IR1) Temperature at the wavelength of IR1 is used for estimating cloud top height. This wavelength corresponds to a so-called "window" of the atmosphere, which means that the radiation emitted from the subject is little absorbed in the atmosphere, hence the observation well describes the temperature of the subject including surface.

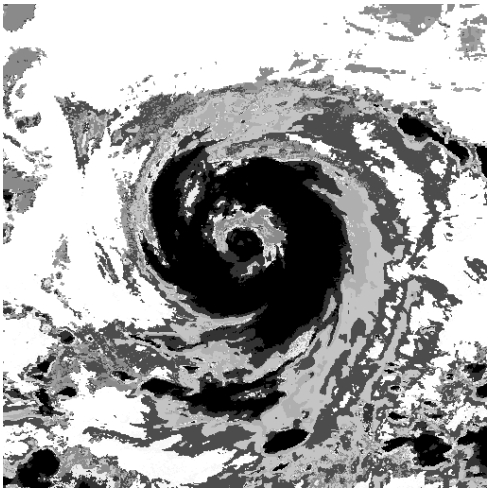

(a) The result of classification

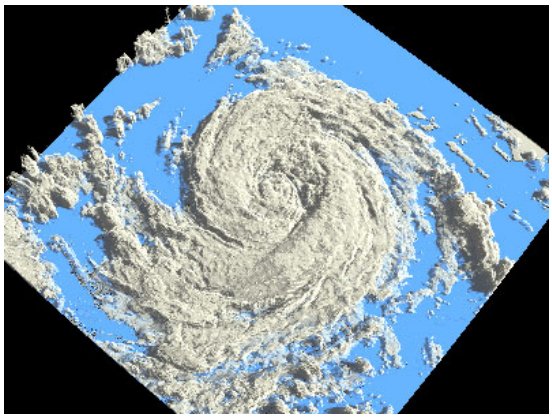

(b) Perspective (oblique) view of a typhoon based on the result of classification (a).

Figure 2: The result of cloud classification. The original image is the same as Figure 1.

TBB(IR1) - TBB(IR2) The wavelength of IR1 and IR2 is next to each other as shown in Table 1, so temperature estimated from these two bands show very similar values. However, relatively small difference indicates convective clouds, fogs, and so on, so this difference can be used for classifying certain types of clouds.

TBB(IR1) - TBB(IR3) Infrared radiation at the wavelength of IR3 is well absorbed by the humid atmosphere. So TBB(IR3) indicates the humidity of upper atmosphere, and this information can be used for classifying certain types of clouds.

4.2.3 Classification of Mixels

One of the big problems in cloud classification is the separation of mixels (mixed pixels) from other pure pixels. Because cirrus is a very thin type of clouds, it often appears as semi-transparent cirrus and the observation of such cloud becomes the mixture of cirrus itself and something below it (middle layer clouds, sea, and so on). Here simple emission equation for cirrus clouds can be represented as follows:

$$R = \varepsilon R_c + (1 - \varepsilon) R_a \tag{1}$$

where ε is the effective cloud emissivity, R_c is the radiance from an opaque cloud (cirrus) and R_a is the upwelling radiance at cloud base. $\varepsilon \sim 1$ for thick cloud but if $\varepsilon < 1$, the observed radiance becomes a mixture of two different types of radiation. Radiance can be directly converted to temperature, so the above equation also indicates the mixture of two types of temperature.

Our proposed algorithm [10, 8] can handle this type of mixels from statistical viewpoint based on the probabilistic model of mixels. This method is incorporated into the proposed classification algorithm as follows.

Basically, to decide whether a pixel is a mixel or a pure pixel, we have to incorporate information from neighboring pixels. For example, if we observe as a pixel value temperature in the middle of the temperature of cirrus and sea, we can imagine that a pixel maybe a middle layer cloud or a mixture of cirrus and sea; however, this information is insufficient to determine which assumption is actually correct. To solve this problem, we look at neighboring $B \times B$ pixels and investigate the variation of pixel values inside the block. If this variation is large, we can decide that this block consists of sea and cirrus pixels.

In the following, due to the limited space, the method is briefly described. When we regard all the B^2 pixels in the block as the mixture of class 1 and class 2, for example the mixture of cirrus (class 1) and sea (class 2), the mean μ_M and the variance σ_M^2 of the pixel values can be calculated as follows:

$$\begin{aligned}
\mu_M &= \frac{1}{\phi_1 + \phi_2}(\phi_1 \mu_1 + \phi_2 \mu_2) \\
\sigma_M^2 &= \frac{1}{(\phi_1 + \phi_2)(\phi_1 + \phi_2 + 1)} \times \\
&\quad \left\{ \phi_1(\phi_1 + 1)\sigma_1^2 + \phi_2(\phi_2 + 1)\sigma_2^2 + \frac{\phi_1 \phi_2}{\phi_1 + \phi_2}(\mu_2 - \mu_1)^2 \right\}
\end{aligned} \tag{2}$$

where ϕ_1 and ϕ_2 is the parameters of Beta distribution for the area proportion distribution, and μ_i and σ_i^2 and is the mean and the variance of class i respectively. Solving Equation (2) with respect to μ_i gives the estimate of mean value of each class:

$$\begin{aligned}
\mu_1 &= \mu_M - \frac{1}{\phi_1} \times \\
&\quad \sqrt{\phi_1(\phi_1 + 1)(\sigma_M^2 - \sigma_1^2) + \phi_2(\phi_2 + 1)(\sigma_M^2 - \sigma_2^2) + 2\phi_1 \phi_2 \sigma_M^2} \\
\mu_2 &= \mu_M + \frac{1}{\phi_2} \times \\
&\quad \sqrt{\phi_1(\phi_1 + 1)(\sigma_M^2 - \sigma_1^2) + \phi_2(\phi_2 + 1)(\sigma_M^2 - \sigma_2^2) + 2\phi_1 \phi_2 \sigma_M^2}
\end{aligned} \tag{3}$$

The above equations suggest that if we know the values of ϕ_i and σ_i^2 from other sources, then we can estimate the mean (mean temperature in this case) of each class from the observed mean and variance of the $B \times B$ block around the pixel. This relationship is used for unmixing the mixture of cirrus and other types.

4.2.4 Classification Results

Figure 2(a) shows the result of classification using our proposed algorithm. Gray scale represents cloud types, but we omit the detail of each class due to the limited space. Note that black regions around the center of the typhoon correspond to cumulonimbus and are called central dense overcast (CDO). This cloud region is very important to estimate the intensity of the typhoon. Moreover, the eye is also recognizable in the heart of CDO, which consists of lower layer clouds such as cumulus.

To give more intuitive understanding of the result of cloud classification, the classification result is visualized in the perspective view in Figure 2(b) by assigning cloud top height and cloud thickness to each pixel. The cloud in the eye seems to be lower than surrounding region containing cumulonimbus that forms central dense overcast.

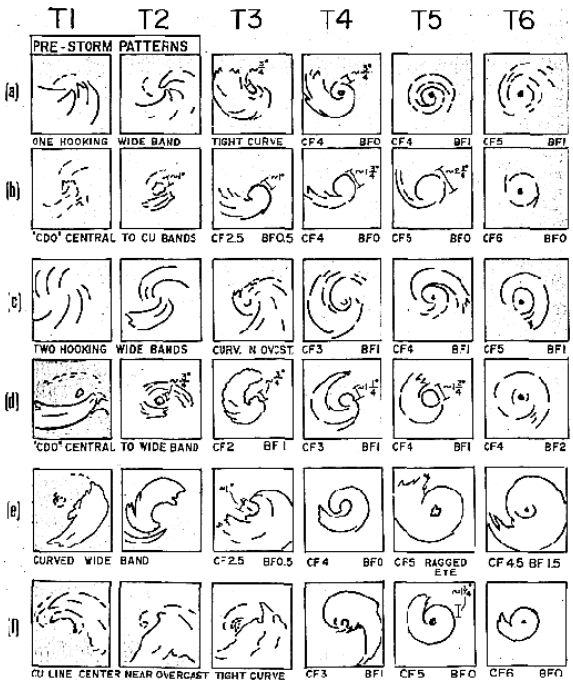

Figure 3: Common tropical cyclone patterns and their corresponding T-numbers. The patterns may be rotated to fit a particular picture of a cyclone. The image taken from [3].

5 Shape Analysis

5.1 Dvorak Method

Dvorak proposed a technique for using satellite pictures to analyze and forecast tropical cyclones [3]. His original method has been extended, and virtually all of the research centers of tropical cyclones utilize extended Dvorak methods for analysis [12]. The analysis mainly relies on three kind of numbers, namely Pattern Tropical number (PT), Data Tropical number (DT), Model Expected Tropical number (MET), and their derivative, T-number.

The underlying assumption of PT is that the current intensity of a typhoon can be estimated by comparing current cloud pattern to average cloud patterns derived from many past typhoons whose intensity is already known. On the other hand, the underlying assumption of DT is that numerical features of cloud patterns such as cloud top height or the length of cloud bands help us estimate the intensity of a typhoon in an objective manner. Moreover, MET focuses on the history of a typhoon; namely, the past change of intensity is compared to the average pattern of daily changes associated with the model of typhoon development.

The derivation of these numbers is currently semi-automatic, but the difficult part of the process, namely pattern recognition, still relies on human intervention. The introduction of pattern recognition techniques into Dvorak method therefore can be expected to improve the analysis of a typhoon in accuracy and speed.

5.2 Shape Decomposition

In this paper, we are especially interested in the analysis of cloud patterns, namely the shape of typhoon clouds. There appear many kinds of shape that should be represented in the typhoon image database, such as spiral shape and band shape. But in this paper, as a starting point, we focus on elliptic shape on typhoon imagery. The usage of ellipse is related to the fact that the clouds around the center of the eye rotate around the centroid because of the centrifugal force. This physical process form rounded elliptic shape, so this shape is expected to be particular important for describing central features (CF) in Dvorak method because this shape characterizes the central area of a typhoon. Therefore, in this paper, we describe typhoon cloud patterns with a set of ellipses. This method is called "shape decomposition," and an ellipse is called decomposition element.

5.3 Deformable Ellipses

We next consider some mechanisms for finding the best fit of decomposition element to complex cloud shape. Our algorithm employed here is inspired by abundant literatures on deformable models [5, 1]. Deformable template is a parametric shape model $r(s, x)$

with relatively few degrees of freedom. The template is matched to an image by searching for the value of the parameter vector x that minimizes a certain energy. Other models with higher degrees of freedom is called snake or active contours, and it is capable of representing much more variety of shape.

The proposed method is a variant of deformable template, where the template is restricted to the ellipse. The shape space of an ellipse can be represented as five-dimensional space $\mathbf{x} = (s, a, \theta, x_c, y_c)$, where the radius of longer axis s, aspect a, the rotation angle of longer axis θ, and the translation of the centroid (x_c, y_c). The problem here is to find the optimal shape vector that maximizes the goodness of fit, or in other words "energy", of the ellipse to the object to be fitted.

Here we denote a set of pixels inside the deformable template Z_i. The energy is calculated by the summation of relevance value S for Z_i. The relevance of each pixel should be given as constraints from outside programs. Typically the relevance of each pixel is assigned according to the classification class of the pixel, or more directly assigned based on the pixel (gray) value itself. In this paper, since we would like to represent the shape of cumulonimbus cloud areas, we assign Cb class a high relevance value, while other cloud classes are assigned low values and the sea class is assigned especially low value (actually minus value).

The positive relevance value serves as a expansive force, while negative relevance value serves as a contractive force. Hence balance between relevance values determine the final shape of the template. Furthermore, we define "penalty" terms as additional constraints. Here we define a set of pixels Z_o and Z_f, which means a set of pixels overlapping with other templates and sticking out of the image frame respectively. Penalty P_o and P_f affects on those sets as contractive force, and we have the final form of the energy:

$$G = \sum_{Z_i \setminus (Z_o \cup Z_f)} S - \sum_{Z_o} P_o - \sum_{Z_f} P_f \qquad (4)$$

The combination of relevance values and penalties determine the stiffness of fitting, and giving too large penalty results in overfitting to the objects.

Finally the goodness-of-fit is maximized by iterative, non-linear gradient descent algorithm called quasi Newton (BFGS) algorithm [13], which will tend to find a good minimum. For the reference, we will briefly describe the initialization phase of the shape vector. In the first place, the location of the decomposition element is estimated from a variant of quad-tree structure using "coarse-to-fine" strategy. Next we calculate the function of distance with respect to angle where distance is measured as one between the center and the (nearest) boundary. Using the smoothed distance function, we can estimate the the scale of axes and rotation angle. There are other minor details to make the description complete, but we omit the detail.

5.4 Motion Analysis and Prediction

Motion analysis is another important aspect in the analysis of typhoons. Usually the motion of clouds are measured by estimating a block-based motion vector. Semiautomatic block matching method is operationally used at JMA, and many kinds of algorithms for computing optical flow can also be applied to this problem [14]. However, without very frequent observations like every one minute (described in [16]), motion vector cannot be estimated accurately from normal hourly observations because of very strong wind whirling around the center of the typhoon.

Then we focus on other types of motions; namely we follow the motion of ellipses extracted by shape decomposition addressed in the previous subsection. An ellipse, which is an approximation of a cloud cluster, moves along time with rotating its axis. Then the velocity of each ellipse can be estimated by comparing the current shape vector to the previous one.

For the tracking of ellipses along a sequence of images, it is a good idea to predict the shape vectors of ellipses in the next time slot from the past estimate. Formally, we represent a shape vector at time T as $\mathbf{x}^T$, and the problem here is to estimate $\mathbf{x}^T$ from the past shape vector $\mathbf{x}^i, (i = 0, \cdots, T-1)$. This is a common problem in motion analysis, and many kinds of methods has been developed. A very simple rule (which we use in the first place) is to use the shape vector estimated on the previous time slot, namely $\mathbf{x}^T = \mathbf{x}^{T-1}$. Another simple rule is the linear extrapolation using the relationship $\mathbf{x}^T - \mathbf{x}^{T-1} = \mathbf{x}^{T-1} - \mathbf{x}^{T-2}$. In general, various prediction methods can be described based on the autoregressive (AR) model, and more advanced methods such as Kalman filtering can be applied to this problem [1].

5.5 Attributed Relational Graph

The spatial relationship between cloud clusters is represented by graph structures, namely attributed relational graphs. This graph structure consists of nodes and edges, where nodes represent the location of a cloud cluster, while edges represent spatial relationship between cloud clusters. Nodes and edges have symbols and (numeric) attributes that characterizes their various properties. Distance between graphs can be calculated by graph matching, and if we interpret this value as the dissimilarity measure between graphs, we can realize similarity-based retrieval of graphs, namely corresponding images.

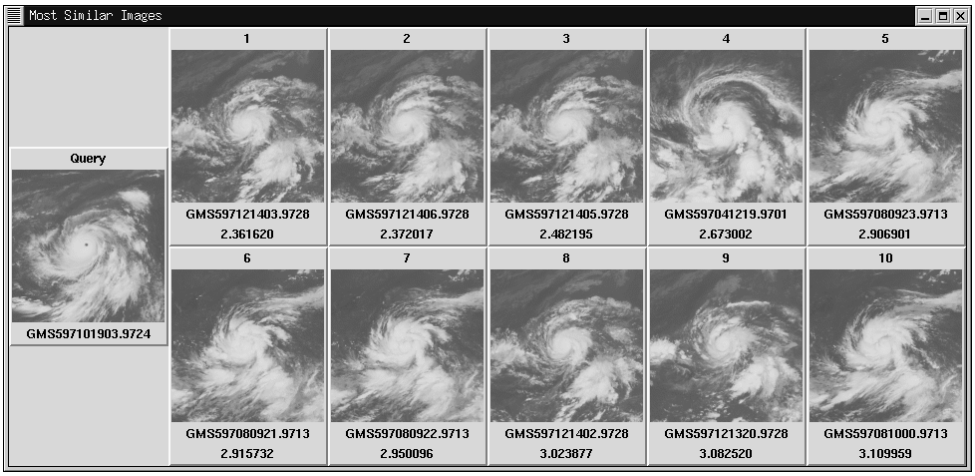

(a) Result of Similarity Retrieval. Query and top 10 similar images. Shown in IR1.

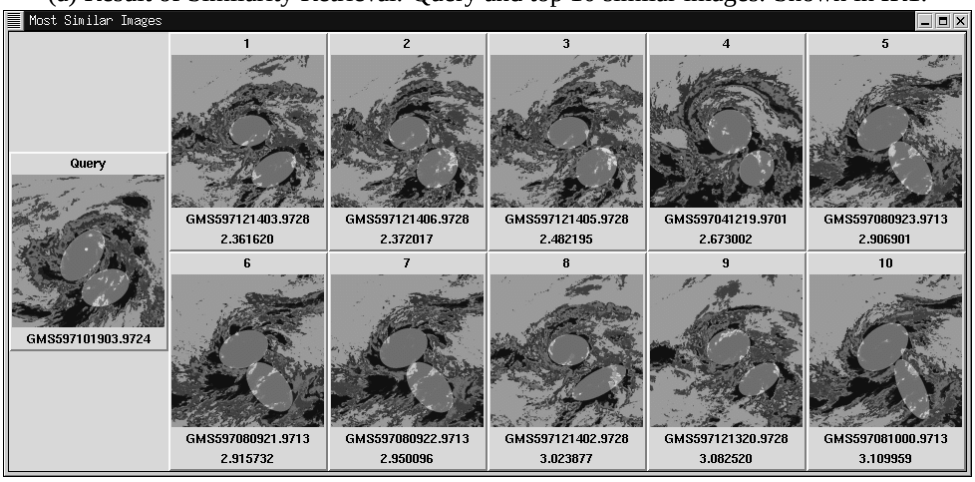

(b) The same result as (a), but shown with decomposition elements

Figure 4: Result of similarity-based image retrieval.

6 Content-Based Search

6.1 Text-Based Retrieval

Satellite images are related to best track dataset that contains central location, central pressure, maximum wind, and so on. Then it is trivial to search images by typhoon number or meteorological elements such as central pressure. Another interesting functionality is to search by track, where similarity is measured by the displacement of track for its whole life cycle or only part of its life. The distance can be measured by means of some metric (Euclid, etc.) using dynamic programming. However, this kind of retrieval methods are actually not new; they are already provided as commercial products or at several web sites.

These alphanumeric data can be much more effectively utilized by combining them with satellite images. For example, if AMeDAS data are combined with satellite images, we can recognize cloud patterns in satellite images, so precipitation caused by the effect of typhoon can be separated from that caused by other cloud systems, and it may be interesting to search typhoon by precipitation pattern.

6.2 Image-Based Retrieval

In addition to text-based retrieval, the focus of this paper is on the development of image-based retrieval methods. In a sense, similarity retrieval of weather charts is a kind of image-based retrieval system [4], but we concentrate on a content-based retrieval of satellite cloud patterns. The advantage of image-based retrieval can be summarized as follows:

1. Alphanumeric data such as central pressure or maximum wind is a very reduced representation of a typhoon, so cloud patterns contain much more information to be relevant in meteorology, such as central features and banding features.

2. Analysis of clouds may reveal mesoscale (small-scale) phenomena which does not clearly appear in alphanumeric data or weather charts.

Currently the system is still under development, and it only provides search functionality based on the graph structure that represents the elliptic shape and spatial relationship of cumulonimbus areas. A user can change weights assigned to features to tell the system which features the user is interested in. The result is sorted based on the similarity measure, and the user can iteratively search the system.

Future development of the system should include the representation of spiral shape and the eye, and should provide search functionality based on the combination of those features. The shape decomposition method developed in this paper cannot be directly used for these kind of features, so we should develop another mechanism for these features.

7 Experiments

We constructed the first prototype database for 28 typhoons born in 1997, whose typhoon number is represented as 97XX (XX is a two digit number from 01 to 28). The number of scenes is 5952 extracted from 3986 original images.

Similarity retrieval experiment is done by selecting the query image randomly and retrieve top 10 images that are most similar to the query. However, if we pick up top 10 images without any filtering, usually typhoon images of the same typhoon whose observation time is close to the query appear as most similar images. So we filter out any images that has the same typhoon number to the query and searches similar cloud patterns from other typhoons. The weights for similarity retrieval are all set to one.

8 Conclusion

This paper introduced a newly developed image database, typhoon image database. This system provides content-based search mechanism based on cloud patterns of typhoons. Nearly 6000 scenes are collected and carefully processed so that this dataset can be used for various purposes. Complex shape and non-rigid motion analysis of cloud patterns is a good subject of research and the author is planning to have many other types of content-based search mechanisms in the system.

Acknowledgement

The author thanks Prof. Kitsuregawa and Dr. Nemoto at Institute of Industrial Science (IIS), University of Tokyo, for providing GMS satellite images used in this paper. He also thanks Prof. Aizawa, Dr. Kodama and Dr. Vuthichai who, as project members, suggested many good ideas at brainstorming meetings.

References

[1] A. Blake and M. Isard. *Active Contours*. Springer, 1998.

[2] M. S. Center. The renewal of GMS-5 system. Technical report, Meteorological Satellite Center, 1996.

[3] V. Dvorak. Tropical cyclone intensity analysis and forecasting from satellite imagery. *Monthly Weather Review*, 103:420–430, 1975.

[4] E. Jones and A. Roydhouse. Intelligent retrieval of archived meteorological data. *IEEE Expert*, 10(6):50–57, 1995.

[5] M. Kass, A. Witkin, and D. Terzopoulos. Snakes : Active coutour models. In *Proc. of 1st ICCV*, pages 259–268, 1987.

[6] S. Kigawa. A mapping method for VISSR date. *Meteorological Satellite Center Technical Note*, (23):15–34.

[7] A. Kitamoto. Toward content-based satellite image database systems over the network. In *The Proceedings of the 5th International Workshop on Academic Information Networks and Systems*, pages 31–38, 1998.

[8] A. Kitamoto. A maximum likelihood thresholding method considering the effect of mixels. *Technical Report of the Institute of Electronics, Information and Communication Engineers*, PRMU99-166:7–14, 1999. (Japanese).

[9] A. Kitamoto and M. Takagi. Hierarchical model as a framework for constructing similarity-based image retrieval systems. *Technical Report of the Institute of Electronics, Information and Communication Engineers*, PRMU97-58:25–32, 1997. (in Japanese).

[10] A. Kitamoto and M. Takagi. Image classification using probabilistic models that reflect the internal structure of mixels. *Patttern Analysis and Applications*, 2(2):31–43, 1999.

[11] D. Longshore. *Encyclopedia of Hurricanes, Typhoons, and Cyclones*. Facts On File, Inc., 1998.

[12] Meteorological Society of Japan. New meteorology — state-of-the-art in understanding of the typhoon, 1999.

[13] W. Press, S. Teukolsky, W. Vetterling, and B. Flannery. *Numerical Recipes in C*. Cambridge University Press, second edition, 1992.

[14] Q. Wu. A correlation-relaxation-labeling framework for computing optical flow — template matching from a new perspective. *IEEE Transactions on Pattern Analysis and Machine Intelligence*, 17(8):843–853, 1995.

[15] M. Yamasaki. *Typhoon*. Tokyo-do Shuppan, 1982. (Japanese).

[16] L. Zhou, C. Kambhamettu, and D. Goldgof. Extracting nonrigid motion and 3D structure of hurricanes from satellite image sequences without correspondences. In *Proc. of IEEE Conference on Computer Vision and Pattern Recognition*, volume II. IEEE, 1999.